Synthesis and Characterization of Non-centrosymmetric $TeSeO_4$

Yetta Porter, N. S. P. Bhuvanesh, and P. Shiv Halasyamani*

Department of Chemistry, University of Houston, 4800 Calhoun Boulevard, Houston, Texas 77204-5641

Received August 31, 2000

The synthesis, crystal structure, and characterization of a non-centrosymmetric oxide, $TeSeO_4$, are reported. The material was synthesized by combining TeO_2 and SeO_2 in a quartz tube and heating at 370 °C. $TeSeO_4$ has a three-dimensional structure containing $[SeO_{3/2}]^+$ cations linked to $[TeO_{5/2}]^-$ anions. Both the Se^{4+} and the Te^{4+} atoms are in asymmetric environments owing to their nonbonded electron pair. The material is SHG active, with a SHG intensity of 400 times SiO_2. Crystal data: monoclinic, space group *Ia* (No. 9, cell choice 3), with $a = 4.3568(8)$ Å, $b = 12.465(3)$ Å, $c = 6.7176(15)$ Å, $\beta = 90.825(4)°$, and $Z = 4$.

Introduction

The design, synthesis, and characterization of new frequency-doubling, second-harmonic generating (SHG), inorganic materials remain a challenge for materials chemists.[1,2] Viable SHG materials must combine chemical and thermal stability with optical transparency and resistance to laser damage. One feature that is required of all SHG materials is crystallographic non-centrosymmetry (NCS).[3] With inorganic materials, this macroscopic NCS is often a manifestation of the asymmetric coordination environments of the metal cations. This asymmetry is a necessary but not sufficient condition to produce crystallographic NCS. That is, the material may crystallize with the asymmetric units aligned in an antiparallel manner, leading to overall crystallographic centrosymmetry. To ascertain if there were any common features among NCS oxides, we reviewed these materials[4] and determined the influence of second-order Jahn−Teller (SOJT) distortions. A SOJT distortion[5−8] is concerned with structural changes attributable to a nondegenerate ground-state interacting with a low-lying excited state. The distortion occurs when the energy gap between the highest occupied (HOMO) and lowest unoccupied (LUMO) molecular orbital is small *and* there is a symmetry-allowed distortion permitting the mixing of the HOMO and LUMO states. Two families of cations in an oxide environment are susceptible to SOJT distortions, d^0 transition metals, e.g., Ti^{4+}, Nb^{5+}, and W^{6+}, and cations with nonbonded electron pairs, e.g., Sb^{3+}, Se^{4+}, and Te^{4+}. For the cations with nonbonded electron pairs an example using Sb^{3+} is illustrative. Four-coordinate Sb^{3+} might be expected to have tetrahedral symmetry (T_d). However, in this geometry the s^2 electron pair would occupy a strongly antibonding a_1* orbital (HOMO). As such, a distortion occurs to distorted square pyramidal geometry (C_{2v}) that lowers the energy of the HOMO by mixing with the LUMO p orbital, i.e., s−p mixing. Thus the HOMO is stabilized and the lone pair becomes sterochemically active, resulting in the asymmetric coordination environment.

One strategy that may be employed to create new NCS materials involves synthesizing oxides that contain cations susceptible to SOJT distortions.[9,10] With this in mind, we have been investigating the synthesis of oxides containing *only* cations with nonbonded electron pairs. The first system we chose to investigate was the Te^{4+}−Se^{4+}−oxide family. Within this family two compounds have been reported, Te_3SeO_8 and $Te_2Se_2O_8$.[11,12] In reviewing the report on $Te_2Se_2O_8$, we noticed some problems with the structure. The reported structure, in *P*1, has two unique Te^{4+} and two unique Se^{4+} cations. Te(1) and Te(2) are in identical coordination environments, as are Se(1) and Se(2). The similar coordination environments for the respective metals strongly suggest higher symmetry. Also, the reported space group, *P*1 (No. 1), is suspect for a three-dimensional oxide material.[13] We resynthesized this material, which should be denoted as $TeSeO_4$. Powder SHG measurements using 1064 nm radiation revealed a strong positive signal; that is, green light was observed, confirming a NCS space group. The strong SHG result suggested that a redetermination of the structure would be appropriate to better understand the relationships between SHG and crystal structure. We were able to grow a single crystal of $TeSeO_4$ and determined the previously reported structure was in error. We report in this paper the synthesis, structure, and characterization of $TeSeO_4$, including infrared, thermogravimetric, and second-order nonlinear optical measurements.

Experimental Section

Synthesis. *Caution!* Use appropriate safety measures to avoid toxic SeO_2 and TeO_2 dust contamination. SeO_2 (0.944 g, 8.51×10^{-3} mol) and TeO_2 (1.181 g, 7.40×10^{-3} mol) were combined, pressed into a pellet, and placed in a quartz tube. Owing to the sublimation of SeO_2, 15% excess was necessary to produce a pure phase product. If 15% excess SeO_2 is not used, a mixture of $TeSeO_4$ and TeO_2 is recovered. The tube was evacuated for several hours and sealed. The tube was held at 370 °C for 3 days and cooled at a rate of 6 °C/h to room

(1) Fejer, M. M. *Phys. Today* **1994**, *36*, 25.
(2) Auciello, O.; Scott, J. F.; Ramesh, R. *Phys. Today* **1998**, *40*, 22.
(3) Nye, J. F. *Physical Properties of Crystals*; Oxford University Press: Oxford, 1957.
(4) Halasyamani, P. S.; Poeppelmeier, K. R. *Chem. Mater.* **1998**, *10*, 2753.
(5) Opik, U.; Pryce, M. H. L. *Proc. R. Soc. (London)* **1957**, *A238*, 425.
(6) Bader, R. F. W. *Mol. Phys.* **1960**, *3*, 137.
(7) Bader, R. F. W. *Can. J. Chem.* **1962**, *40*, 1164.
(8) Pearson, R. G. *J. Mol. Structure (THEOCHEM)* **1983**, *103*, 25.
(9) Halasyamani, P. S.; O'Hare, D. *Inorg. Chem.* **1997**, *36*, 6409.
(10) Halasyamani, P. S.; O'Hare, D. *Chem. Mater.* **1997**, *10*, 646.
(11) Pico, C.; Castro, A.; Viega, M. C.; Gutierrez-Puebla, E.; Monge, M. A. *J. Solid State Chem.* **1986**, *63*, 172.
(12) Delange, C.; Carpy, A.; Gourselle, M. *C. R. Acad. Sci. Paris* **1982**, *295*, 981.
(13) Marsh, R. E. *Acta Crystallogr.* **1995**, *B51*, 897.

10.1021/ic000994u CCC: $20.00
Published on Web 02/10/2001

Table 1. Crystallographic Data for $TeSeO_4$

fw = 270.56	$Z = 4$
space group *Ia* (No. 9, cell choice 3)	$T = 293$ K
$a = 4.3568(9)$ Å	$\lambda = 0.71073$ Å
$b = 12.465(3)$ Å	$\rho = 4.927$ g/cm^3
$c = 6.7176(15)$ Å	$\mu = 179.84$ cm^{-1}
$\beta = 90.825(4)°$	$R(F)^a = 0.027$
$V = 364.77(14)$ Å^3	$R_w(F^2)^b = 0.067$

^{a} $R = \sum||F_o| - |F_c||/\sum|F_o|$. ^{b} $R_w = [\sum w(|F_o^2| - |F_c^2|)^2/\sum w(F_o^2)^2]^{1/2}$.

Table 2. Atomic Coordinates for $TeSeO_4$

atom	*x*	*y*	*z*	U(eq)^a (Å^2)
Te	0.5107	0.6116(1)	0.9237	0.0107(2)
Se	0.2481(3)	0.8783(1)	0.9301(2)	0.0143(3)
O(1)	0.525(2)	0.6145(5)	0.6194(15)	0.018(2)
O(2)	0.508(3)	0.6014(7)	0.248(2)	0.036(3)
O(3)	0.1151(12)	0.5471(4)	0.9155(10)	0.016(1)
O(4)	0.1761(13)	0.7461(4)	0.9185(11)	0.021(1)

^{a} U(eq) is defined as one-third of the trace of the orthogonalized U_{ij} tensor.

temperature. From the resultant off-white powder, a clear colorless prismatic crystal was manually extracted. Powder X-ray diffraction on the remaining material resulted in good agreement with the simulated powder pattern for $TeSeO_4$ (see Supporting Information). The material is slightly moisture sensitive and should be stored in a desiccator.

Structure Determination. Single Crystal. The structure of $TeSeO_4$ was determined by standard crystallographic methods. A clear colorless prismatic crystal (dimensions 0.04 × 0.06 × 0.10 mm) was glued on a thin glass fiber, and room-temperature intensity data were collected on a Siemens SMART diffractometer equipped with a 1K CCD area detector using graphite-monochromated Mo Kα radiation. A hemisphere of data was collected using a narrow-frame method with scan widths of 0.30° in omega and an exposure time of 25 s/frame. The first 50 frames were remeasured at the end of the data collection to monitor instrument and crystal stability. The maximum correction applied to the intensities was <1%. The data were integrated using the Siemens SAINT program,[14] with the intensities corrected for Lorentz, polarization, air absorption, and absorption attributable to the variation in the path length through the detector faceplate. ψ-scans were used for the absorption correction on the hemisphere of data. The crystal structure of $TeSeO_4$ was solved in space group *Ia* (No. 9, cell choice 3) with initial heavy-atoms positions, tellurium and selenium, located by direct methods using SHELXS.[15] This monoclinic cell choice resulted in a β value much closer to 90°. The oxygen atoms were located by subsequent cycles of refinements and Fourier difference maps. The final full-matrix least-squares refinement[16] was against F_o^2 and included anisotropic thermal parameters for all atoms. The final refinement was based on 645 reflections and 56 parameters and converged with $R(F) = 0.027$, $R_w(F) = 0.067$ (Flack parameter 0.00(2)). All calculations were performed using the WinGX-98[17] crystallographic software package. Crystallographic data, atomic coordinates and thermal parameters, and select bond distances and angles for $TeSeO_4$ are given in Tables 1−3, respectively.

Infrared Measurements. Infrared spectra were recorded on a Matteson FTIR 5000 spectrometer in the 400−4000 cm^{-1} range, with the sample pressed between two KBr pellets.

Thermogravimetric Measurements. Thermogravimetric analyses were carried out in air at a heating rate of 5 °C/min to 600 °C using a Seiko 320 TG/DTA operating under static air.

(14) *SAINT*, Version 4.05; Siemens Analytical X-ray Systems, Inc.: Madison, WI, 1995.
(15) Sheldrick, G. M. *SHELXS-97−A program for automatic solution of crystal structures*; University of Goettingen: Goettingen, Germany, 1997.
(16) Sheldrick, G. M. *SHELXL-93−A program for crystal structure refinement*; University of Goettingen: Goettingen, 1993.
(17) Farrugia, L. J. *WinGX: An integrated system of publically available windows programs for the solution, refinement, and analysis of single-crystal X-ray diffraction data*; University of Glasgow: Scotland, 1998.

Table 3. Selected Bond Distances (Å) and Angles (deg) for $TeSeO_4$[a]

Se−O(1)	1.742(10)	O(1)−Se−O(4)	102.2(3)
Se−O(2)	1.697(13)	O(1)−Se−O(2)	93.2(6)
Se−O(4)	1.678(5)	O(2)−Se−O(4)	103.8(9)
Te−O(1)	2.046(10)	O(1)−Te−O(2)	177.3(3)
Te−O(2)	2.183(14)	O(3)−Te−O(3)#1	77.9(1)
Te−O(3)	1.902(5)	O(3)−Te−O(4)	74.0(2)
Te−O(3)#1	2.030(5)	O(3)#1−Te−O(4)	151.9(2)
Te−O(4)	2.222(5)		

[a] Symmetry transformations used to generate equivalent atoms: #1 $x+1/2, -y+1, z$.

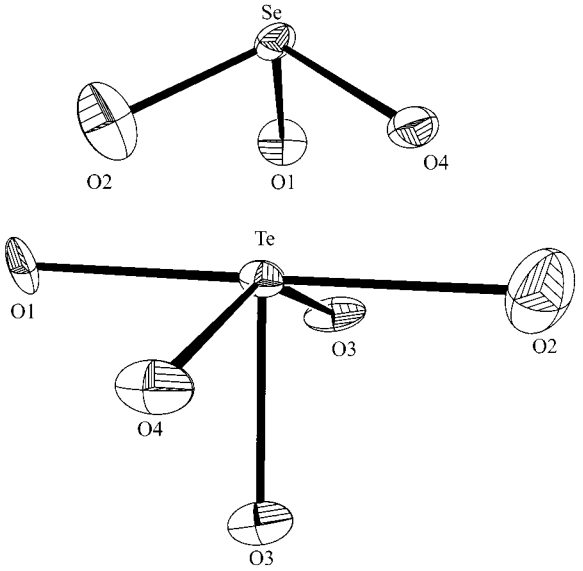

Figure 1. ORTEP (50% probability ellipsoids) of the (a) SeO_3 and (b) TeO_5 moieties.

Second-Order Nonlinear Optical Measurements. Powder SHG measurements were performed on a modified Kurtz-NLO[18] system using 1064 nm light. A Continuum Minilite II laser, operating at 15 Hz, was used for all measurements. Since the SHG efficiency of powders has been shown to depend strongly on particle size,[18,19] polycrystalline $TeSeO_4$ was ground and sieved (Newark Wire Cloth Company) into distinct particle size ranges, < 20 μm, 20− 45 μm, 45−63 μm, 63−75 μm, 75− 90 μm, 90−125 μm, and 125−138 μm. To make relevant comparisons with known SHG materials, crystalline SiO_2 was also ground and sieved into the same particle size ranges. All of the powders were placed in separate capillary tubes. The SHG, i.e., 532 nm green light, radiation was collected in reflection and detected by a photomultiplier tube (Oriel Instruments). To detect only the SHG light, a 532 nm narrow band-pass interference filter was attached to the tube. A digital oscilloscope (Tektronix TDS 3032) was used to view the SHG signal.

Results

Crystal Structure of $TeSeO_4$. $TeSeO_4$ is a ternary Te^{4+}/Se^{4+} oxide containing TeO_5 and SeO_3 units connected by Se−O−Te and Te−O−Te bonds. Interestingly, there are no Se−O−Se bonds. The asymmetric unit contains one unique selenium, one unique tellurium, and four unique oxygen atoms. The selenium atom is in a distorted trigonal pyramidal coordination environment, bonded to three oxygen atoms (see Figure 1a). The Se−O distances range from 1.680(4) to 1.732(9) Å, with O−Se−O angles ranging from 90.9(1)° to 106.7(7)°. Each tellurium atom is in a distorted square pyramidal coordination environment, bonded to five oxygen atoms (see Figure 1b). The

(18) Kurtz, S. K.; Perry, T. T. *J. Appl. Phys.* **1968**, *39*, 3798.
(19) Dougherty, J. P.; Kurtz, S. K. *J. Appl. Crystallogr.* **1976**, *9*, 145.

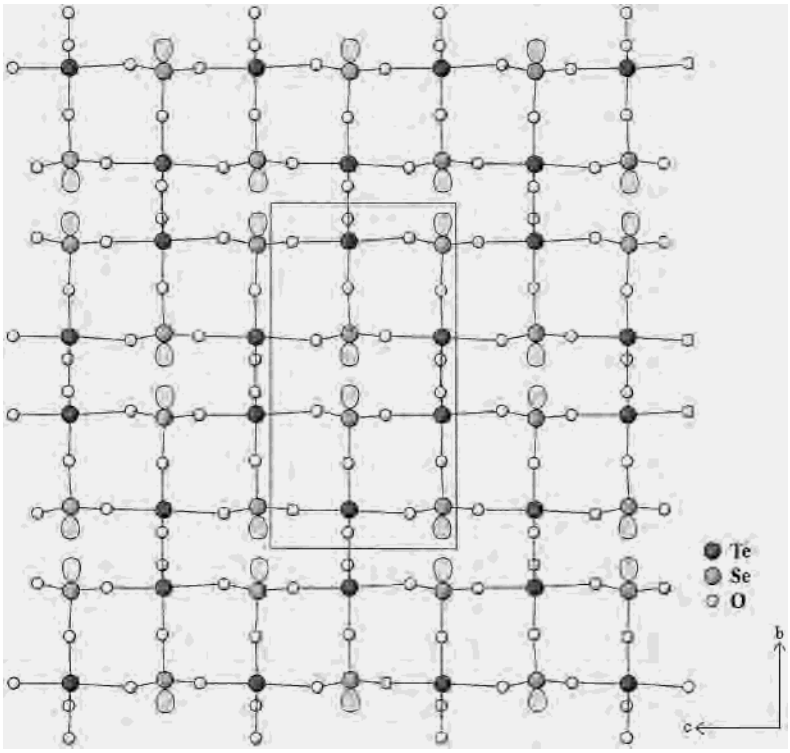

Figure 2. Ball-and-stick diagram of $TeSeO_4$. Note the neutral four polyhedral sequence, $\{[SeO_{3/2}]^+[TeO_{5/2}]^-[TeO_{5/2}]^-[SeO_{3/2}]^+\}^0$, along the [010] direction. The lone pair on Se^{4+} is drawn schematically.

Te−O distances range from 1.901(5) to 2.222(5) Å, with O−Te−O angles ranging from 74.1(2)° to 176.5(8)°. The bond distances and angles are similar to those in Te_3SeO_8.[11] Each oxygen around the selenium atom is bonded to a tellurium, whereas for the tellurium, of the five oxygen atoms, three are bonded to selenium and two are linked to additional tellurium atoms. Thus in connectivity terms, the SeO_3 and TeO_5 moieties may be formulated as a $[SeO_{3/2}]^+$ cations and $[TeO_{5/2}]^-$ anions, respectively. Bond valence calculations[20,21] on $TeSeO_4$ resulted in values of 3.99 for Se^{4+} and 4.01 for Te^{4+}.

The $[SeO_{3/2}]^+$ cations and $[TeO_{5/2}]^-$ anions link to form a three-dimensional structure (see Figure 2). If the nonbonded electron pair is considered to form part of the polyhedra, the structure can be described as zigzag chains of TeO_5E octahedra running along the [100] direction, with the SeO_3E tetrahedra bridging these chains through sharing all three oxygen atoms along the [010] and [001] directions (see Supporting Information). One of the most interesting structural features of $TeSeO_4$ is observed along the [010] direction. A neutral four polyhedral sequence is observed, $\{[SeO_{3/2}]^+[TeO_{5/2}]^-[TeO_{5/2}]^-[SeO_{3/2}]^+\}^0$, which are separated from one another by the lone pair on the Se^{4+}. Along the [100] direction are double rows of $[TeO_{5/2}]^-$ anions that are connected by $[SeO_{3/2}]^+$ cations, whereas along the [001] direction the polyhedra alternate between $[SeO_{3/2}]^+$ cations and $[TeO_{5/2}]^-$ anions. Thus each $[SeO_{3/2}]^+$ cation is surrounded by three $[TeO_{5/2}]^-$ anions, whereas each $[TeO_{5/2}]^-$ anion is connected to three $[SeO_{3/2}]^+$ cations and two additional $[TeO_{5/2}]^-$ anions.

Infrared Measurements. The IR spectrum revealed stretches consistent with Se−O (833 and 715 cm^{-1}), Te−O (650 cm^{-1}), and Se−O−Te and Te−O−Te (492 and 488 cm^{-1}, respectively) vibrations. These values are in good agreement with those reported previously.[12,22]

Thermogravimetric Measurements. TGA measurements on $TeSeO_4$ in static air revealed one transition at approximately 320 °C corresponding to a weight loss of 41.3%. This value agrees well with the calculated weight loss of 41.0% determined from the reaction $TeSeO_4 \rightarrow TeO_2 + SeO_2\uparrow$. (*Caution*: SeO_2 vapors are poisonous and should be vented with extreme care.) Powder X-ray diffraction measurements on the remaining powder was consistent with TeO_2. It should be noted that no phase transition(s) were observed up to the decomposition temperature, suggesting the material is pyroelectric rather than ferroelectric.

Second-Order Nonlinear Optical Measurements. SHG measurements were performed on sieved powder samples of $TeSeO_4$ and SiO_2. Each sample was placed in a separate capillary tube. Several measurements were taken in order to ensure reproducibility. On the basis of these experiments, we determined that $TeSeO_4$ has a SHG efficiency of 400 times SiO_2.

Discussion

$TeSeO_4$ represents an example of an oxide containing only cations with nonbonded electron pairs. As previously stated, the existence of the stereoactive lone pairs can be understood through a second-order Jahn−Teller distortion. The lone pairs strongly influence both the structural topology and the SHG behavior. The lone pair on the Se^{4+} cation has a large component in the [010] direction. Structurally, this has the effect of separating the neutral four polyhedral motif, $\{[SeO_{3/2}]^+[TeO_{5/2}]^-[TeO_{5/2}]^-[SeO_{3/2}]^+\}^0$, shown in Figure 2. The lone pair on the Te^{4+} is directed more along the [100] direction. Here, the structural effect is to increase the distance between the $[TeO_{5/2}]^-$ anions along the [100] direction. One of the most important consequences of the lone pairs is the structural non-centrosymmetry. The lone pair creates an inherently acentric environment for both the $Se^{4+}O_3$ and $Te^{4+}O_5$ groups. These groups are linked together in a three-dimensional manner that creates macroscopic acentricity.

(20) Brown, I. D.; Altermatt, D. *Acta Crystallogr.* **1985**, *B41*, 244.
(21) Brese, N. E.; O'Keeffe, M. *Acta Crystallogr.* **1991**, *B47*, 192.
(22) Bart, J. C. J.; Petrini, G. *Z. Anorg. Allg. Chem.* **1984**, *509*, 183.

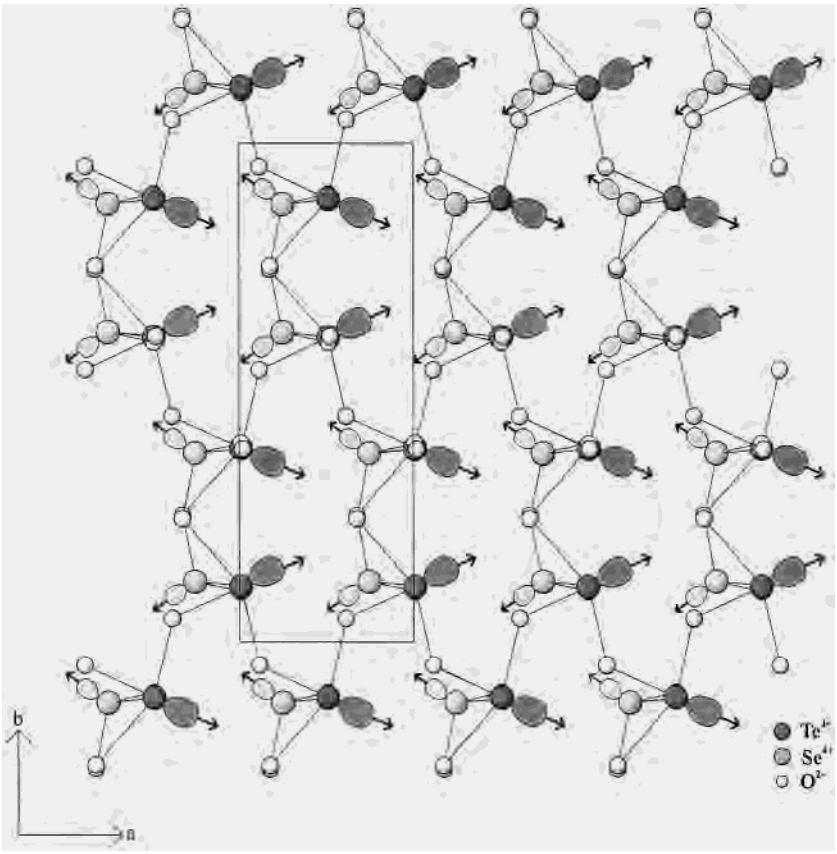

Figure 3. Ball-and-stick diagram of $TeSeO_4$. The lone pairs on the Se^{4+} and Te^{4+} are drawn schematically. The arrows indicate the approximate magnitude and direction of the dipole moments on the SeO_3 and TeO_5 moieties.

An equally important consequence of the stereoactive lone pair is their influence on the SHG behavior. The idea of synthesizing new SHG materials by utilizing metal cations with nonbonded electron pairs has been suggested earlier.[23] These researchers investigated iodates, $MI^{5+}O_3$ (M = alkali metal or NH_4^+), and tellurates, $M'Te^{4+}O_3$ (M′ = alkaline earth or transition metal). With both families of compounds, the researchers noted a high incidence of acentricity through powder SHG measurements. Additionally, calculations by Chen et al.[24,25] have shown that anionic groups containing stereoactive lone pairs, e.g., $(IO_3)^-$ and $(SbF_5)^{2-}$, have larger bond hyperpolarizabilites by one order of magnitude than anionic groups lacking the lone pair, e.g., $(PO_4)^{3-}$. One issue that must be addressed is the influence of the lone pair on the local dipole moment of the anionic group. For metal cations with nonbonded electron pairs, specifically I^{5+}, the direction of the dipole moment is in the direction of the lone pair.[26] In $TeSeO_4$, the dipole moments for both Se^{4+} and Te^{4+} lie in the $a-b$ plane and point in directions approximately $\pm 40°$ and $\pm 25°$ relative to the *a*-axis, respectively. However, the dipole moments point in opposite directions along the [100] direction, $-\mathbf{a}$ for Se^{4+} and $+\mathbf{a}$ for Te^{4+}. For each metal cation, the dipole moments constructively add. This may be understood by a straightforward vector argument. The arrows in Figure 3 indicate the approximate directions of the dipole moment on Se^{4+} and Te^{4+}, respectively. Although there is some cancellation of the dipole moments, i.e., polarization, between SeO_3E and TeO_5E groups, $TeSeO_4$ has a net polarization along the [100] direction owing to the larger dipole moment associated with the TeO_5E group. It is attributable to this net polarization that we observe a substantial SHG response, approximately 400 times SiO_2.

Conclusion

We have succeeded in resynthesizing and characterizing $TeSeO_4$, a NCS oxide containing only cations with nonbonded electron pairs. The material contains $Se^{4+}O_3E$ and $Te^{4+}O_5E$ polyhedra that are inherently acentric. When these polyhedra are linked together in a three-dimensional manner, macroscopic NCS is generated. Powder SHG measurements on $TeSeO_4$ revealed a doubling efficiency of approximately 400 times SiO_2. We plan on investigating further the NLO behavior by utilizing different wavelengths, as well as exploring the synthesis of additional compounds in this and other systems containing cations with nonbonded electron pairs.

Acknowledgment. We acknowledge Dr. James Korp for technical assistance with the X-ray crystallography. We thank the Robert A. Welch Foundation for support. This work used the MRSEC/TCSUH Shared Experimental Facilities supported by the National Science Foundation under Award No. DMR-9632667 and the Texas Center for Superconductivity at the University of Houston.

Supporting Information Available: The following are available: X-ray crystallographic file, in CIF format, experimental and calculated powder X-ray diffraction pattern for $TeSeO_4$, infrared spectrum, thermogravimetric curve, and polyhedral representations of $TeSeO_4$. This material is available free of charge via the Internet at http://pubs.acs.org.

IC000994U

(23) Bergman, J. G.; Boyd, G. D.; Ashkin, A.; Kurtz, S. K. *J. Appl. Phys.* **1969**, *40*, 2860.
(24) Chen, C. T.; Luo, Z. D.; Lin, Z. Y.; Chen, X. S. *Commun. Fujian Inst. Struct. Mater.* **1979**, *2*, 1.
(25) Chen, C.; Liu, G. *Annu. Rev. Mater. Sci.* **1986**, *16*, 203.
(26) Bergman, J. G.; Crane, G. R. *J. Chem. Phys.* **1973**, *60*, 2470.